



# 1 Monetizing the role of water in sustaining watershed ecosystem 2 services using a fully integrated subsurface–surface water model

3 Tariq Aziz<sup>1,2,\*</sup>, Steven K. Frey<sup>1,3</sup>, David R. Lapen<sup>4</sup>, Susan Preston<sup>5</sup>, Hazen A. J. Russell<sup>6</sup>, Omar  
4 Khader<sup>1,7</sup>, Andre R. Erler<sup>1</sup>, Edward A. Sudicky<sup>1,3</sup>

5 <sup>1</sup>Aquanty, 600 Weber St. N., Unit B, Waterloo, ON, N2V 1K4, Canada

6 <sup>2</sup>Ecohydrology Research Group, Water Institute and Department of Earth and Environmental Sciences, University of  
7 Waterloo, Waterloo, N2L 3G1, ON, Canada

8 <sup>3</sup>Department of Earth and Environmental Sciences, University of Waterloo, Waterloo, N2L 3G1, ON, Canada

9 <sup>4</sup>Agriculture and Agri-Food Canada, Ottawa Research and Development Centre, Ottawa, Ontario, Canada

10 <sup>5</sup>Environment and Climate Change Canada, Ottawa, Ontario, Canada

11 <sup>6</sup>Geological Survey of Canada, 601 Booth St., Ottawa, ON, K1A 0E8, Canada

12 <sup>7</sup>Department of Water and Water Structural Engineering, Zagazig University, AlSharqia, Egypt

13 \*Correspondence to: Tariq Aziz (taziz@aquanty.com)

14 **Abstract.** Water is essential for all ecosystem services, yet a comprehensive assessment of total (overall) water  
15 contributions to ecosystem services production has never been attempted. Quantification of the many ecosystem  
16 services impacted by water demands integrated hydrological simulations that implicitly characterize subsurface and  
17 surface water exchange. In this study, we use a fully integrated hydrological model—HydroGeoSphere (HGS)—to  
18 capture changes in subsurface water, surface water, and evapotranspiration (green water) combined with the economic  
19 valuation approach to assess ecosystem services over an 18-year period (2000-2017) in a mixed-use but predominantly  
20 agricultural watershed in eastern Ontario, Canada. Using the green water volumes and ecosystem services values as  
21 inputs, we calculate the marginal productivity of water, which is \$0.45 per m<sup>3</sup> (in 2022 Canadian dollars). The  
22 valuation results show that maximum green water is used during the dry years, with a value of \$1.16 billion during a  
23 severe drought that struck in 2012. The average product of water for ecosystem services declines during the dry years.  
24 Because subsurface water is a major contributor to the green water supply, it plays a critical role in sustaining  
25 ecosystem services during drought conditions. For instance, during the 2012 drought, the subsurface water  
26 contribution to green water was estimated at \$743 million, making up 72% of the total value of green water used in  
27 that year. Conversely, the surface water contributions in green water provision over the modeling period are  
28 comparatively miniscule. This study informs watershed management on the sustainable use of subsurface water during  
29 droughts and provides an improved methodology for watershed-based integrated management of ecosystem services.

## 30 1 Introduction

31 The role of subsurface water (groundwater and soil water in the vadose zone) in socio-economic development is  
32 widely acknowledged (Foster and Chilton, 2003); its ecological contributions are, however, undervalued (Yang and  
33 Liu, 2020), despite being fundamental to the control of terrestrial ecological processes (Qiu et al., 2019). Subsurface  
34 water supports a potpourri of ecosystem services that range from provisioning to regulating, supporting, and cultural  
35 services (Griebler and Avramov, 2015). While water infiltration is a driver for subsurface water recharge, subsurface



36 water discharge is in-turn key for supporting terrestrial ecosystems (e.g., wetlands, forests, etc.) (Griebler and  
37 Avramov, 2015). Hence, subsurface water provides a buffer against weather stressors on vegetation and aquatic  
38 ecosystems and helps to maintain key processes that underpin ecosystem services (Qiu et al., 2019). To date, most  
39 ecosystem services research has focused on aboveground factors and processes (e.g., land use change), and very little  
40 focus has been given to the critical zone (e.g., shallow groundwater) and its influence on terrestrial ecosystem services  
41 (Richardson and Kumar, 2017; Qiu et al., 2019). In a few instances, previous research (e.g., Booth et al., 2016; Li et  
42 al., 2014) has attempted to link subsurface water with land cover, but only at a field scale and under static  
43 environmental conditions (Qiu et al., 2019). Given the difficulties with mapping large/watershed scale subsurface  
44 water resources, the contribution of subsurface water towards terrestrial ecosystem services has rarely been quantified.  
45 Furthermore, monetary/economic valuation of subsurface water contribution to terrestrial ecosystem services has  
46 never been attempted.

47 While hydrologic ecosystem services studies are common in the literature (Ochoa and Urbina-Cardona, 2017),  
48 groundwater-focused ecosystem services assessments have rarely been undertaken. However, groundwater can be an  
49 important regulator of watershed hydrologic behavior and ecosystem health, especially in regions with a shallow water  
50 table, such as the Great Lakes Basin (Neff et al., 2005). In addition, the groundwater acts as a soil water source in  
51 areas of shallow water table (Chen and Hu, 2004). The importance of groundwater has been noted by Griebler and  
52 Avramov (2015) in their review of groundwater ecosystem services, where they highlight that groundwater plays a  
53 direct role in supplying different types of ecosystem services (Millenium Ecosystem Assessment (MEA), 2005); and  
54 they stress the need for a better quantitative understanding of groundwater processes in order to protect and manage  
55 groundwater ecosystem services. Furthermore, Mammola et al. (2019) emphasize that subterranean ecosystems are  
56 largely being overlooked in conservation policies. Based on a preliminary assessment of all the regions around the  
57 world where groundwater plays a critical role in ecosystem services (considering that 43 % of consumptive irrigation  
58 is sourced from groundwater (Siebert et al., 2010)), one has to wonder if the lack of focus on subsurface water  
59 ecosystem services is not due to lack of need, but in fact a lack of tools with which to conduct the required analysis.  
60 Using advanced hydrological models is a convenient approach to completely characterize all water storage and flux  
61 dynamics over large spatial scales. With groundwater ecosystem services' increasing role in policy-making (Honeck  
62 et al., 2021) and sustainable groundwater resources management, additional tools are required in order to map them  
63 more accurately. At present, numerous modeling tools are available for ecosystem services mapping, such as



64 Artificial Intelligence for Environment & Sustainability (ARIES), Co\$ting Nature, Envision, and Integrated  
65 Valuation of Ecosystem Services and Tradeoffs (InVEST), with InVEST being by far the most prominent in the  
66 scientific literature (Ochoa and Urbina-Cardona, 2017). The only approach to completely characterize all water storage  
67 and flux dynamics over large spatial scales is through the use of sophisticated hydrological models. For mapping  
68 hydrological ecosystem services, it is essential to understand and capture complex hydrological processes (Sun et al.,  
69 2017). However, ecosystem services specific models, such as the InVEST Water Yield Model, have limited capability  
70 to simulate hydrological processes efficiently (Redhead et al. 2016). The hydrologic tools built into the ecosystem  
71 services models are usually focused on one water compartment and/or are too simplistic to properly characterize  
72 hydrologically mediated ecosystem services (Dennedy-Frank et al., 2016; Vigerstol and Aukema, 2011). Still, models  
73 like SWAT and many other hydrological models, such as Variable Infiltration Capacity (VIC) and Finite Element  
74 subsurface FLOW (FEFLOW) models, are unable to simulate integrated subsurface-surface water systems. Within  
75 the hydrologic modelling community, it is acknowledged that structurally complex, fully-integrated subsurface–  
76 surface water models are the current state-of-the-art for capturing the interplay between subsurface and surface water  
77 systems, however, this class of models has not yet been applied towards ecosystem services valuation.

78 Another key hydrological and ecological process is evapotranspiration, which can be largely supported by the  
79 availability of groundwater (Jin et al., 2017; Condon et al., 2020). Changes in evapotranspiration rates determine water  
80 availability and ecosystem health at a watershed scale (Zhao et al., 2022). Thus, subsurface water availability is vital  
81 for ecosystem functioning and subsequent ecosystem services. Under drought conditions, subsurface water can  
82 become critically important for sustaining evapotranspiration (Condon et al., 2020). Therefore, mapping the  
83 connection between subsurface water and evapotranspiration is imperative for sustainable water and ecosystem  
84 services management (Yang et al., 2015), especially in cases where growing climate variability is expected to result  
85 in increasingly erratic precipitation patterns (Taylor et al., 2013). A few of the current hydrological models can weakly  
86 capture the subsurface water dynamics and subsurface-surface water interactions (Clark et al., 2015). Because  
87 HydroGeoSphere (HGS) is an integrated subsurface-surface model, it can be used to dynamically integrate key  
88 components of the terrestrial hydrologic cycle such as evaporation from bare soil and water bodies, vegetation-  
89 dependent transpiration with root uptake, snowmelt and soil freeze/thaw dynamics.

90 Evapotranspiration represents large fluxes of both water and energy across the land surface–atmosphere boundary and  
91 is closely related to terrestrial ecosystem production (Tan et al., 2021). Water managers perceive evapotranspiration



92 as a water loss; however, it is an essential process for regulating the hydrologic cycle and providing terrestrial  
93 ecosystem services (An and Verhoeven, 2019). Evapotranspiration is also called green water—the fraction of the  
94 rainfall on the land that eventually returns to the atmosphere as evapotranspiration—which is a source of nutrition for  
95 vegetation/ecosystems and plays a key role in producing ecosystem services (Zisopoulou et al., 2022; Schyns et al.,  
96 2019). Green water is evapotranspired during biomass production, and thus supports and maintains terrestrial  
97 ecosystems (Lowe et al., 2022). Hence, evapotranspiration is pivotal in the growth and functioning of ecosystems (Liu  
98 and El-Kassaby, 2017) and plays a major role in providing ecosystem services through biomass production. It is also  
99 a key process by which to model/map terrestrial ecosystem services production. To capture the interaction between  
100 evapotranspiration and subsurface and surface waters, fully-integrated subsurface–surface water models are well  
101 suited.

102 In this study, we introduce the HydroGeoSphere (HGS), a fully-integrated subsurface– surface water model, as a tool  
103 for mapping and quantifying subsurface and surface water contributions to terrestrial ecosystem services at the  
104 watershed scale (~4000 km<sup>2</sup>). Furthermore, the results from the HGS modelling are extended to an economic valuation  
105 of water contributions to ecosystem services. Until now, fully integrated subsurface-surface models such as HGS have  
106 not been demonstrated in the scientific literature as tools for modeling ecosystem services, and the economic value of  
107 subsurface water has been overlooked in ecosystem services valuation assessments. To address this omission, we  
108 demonstrate the model for a watershed in a humid temperate climate in eastern Ontario, Canada, with a generally  
109 shallow (1-3m) water table. Furthermore, using the simulation results, we value the contribution of subsurface and  
110 surface water storages to evapotranspiration and subsequently to terrestrial ecosystem services. As such, the work  
111 herein provides an important and novel contribution to the science of ecosystem service valuation in terms of both  
112 conceptual and methodological understanding. This work identifies the level of complexity required in a model to  
113 quantify water ecosystem services, especially from shallow water regions.

## 114 **2 Materials and Methods**

### 115 **2.1 Study Area**

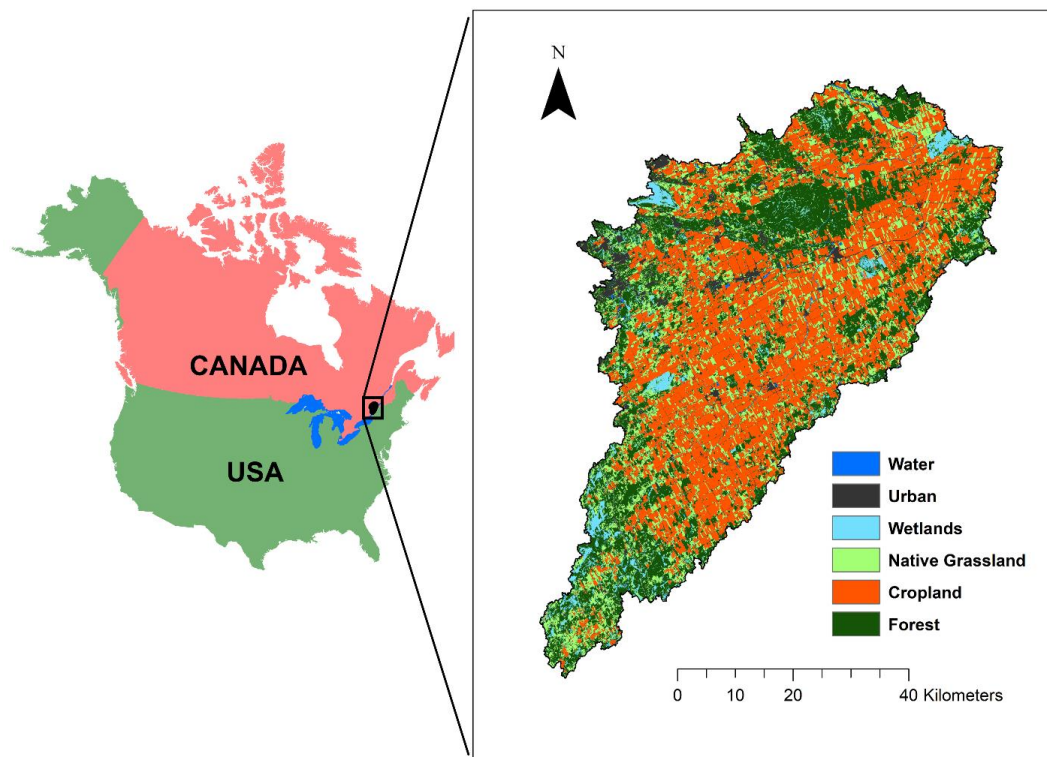
116 The South Nation watershed (SNW), located in eastern Ontario, Canada, covers approximately 3,830 km<sup>2</sup> (Fig. 1).  
117 There is approximately 100 m of vertical relief in the land surface, and the relief is relatively flat (Fig. 1A). It is  
118 primarily an agriculture-focused watershed, with relatively low population density. The towns of Casselman, Russell,



119 and Winchester have respective populations of 3,548, 16,520 and 2,394 based on the 2016 Canada census. The eastern  
120 flank of the city of Ottawa is encroaching on the Northwest corner of the watershed, in many headwater areas. The  
121 SNW stream network is approximately 6,489 km long and consists of 1,606 km of Strahler order 3+, 1,548 km of  
122 Strahler order 2, and 3,335 km of Strahler order 1 features (Fig. 2A). Many of the low order features are either  
123 completely manmade agricultural drainage ditches, or straightened natural watercourses designed to drain the  
124 agricultural landscape.

125 Soil drainage conditions across the watershed are primarily imperfect, poor, or very poor (Fig. 3A), although some  
126 disconnected pockets are considered well drained (SLC, 2010). The wide extent of poorly drained soils in the SNW  
127 is an integral reason for the intensive land drainage activities. Tile drainage is extensively employed to enhance  
128 agricultural productivity and to facilitate cropping activities in these soils. Approximately 960 km<sup>2</sup> (or 25 %) of the  
129 watershed is tile-drained (Fig. 4A). From 2004 to 2016, 290 km<sup>2</sup> of land was tile drained. Across most of the SNW,  
130 the soils are underlain by Quaternary deposits, primarily of glacial, glacial marine, fluvial, and colluvial origin  
131 (Ontario Geological Survey, 2010). These sediments are composed of sand, silt, clay, gravel, and glacial till, and range  
132 in thickness from 0 m to approximately 90 m across the watershed. Eight soils have been identified in the SNW (SLC,  
133 2010), mainly composed of clay loam and sandy loam textures (Fig. 3A(a)). Localized areas associated with incised  
134 bedrock channels and Quaternary esker deposits are important sources of groundwater for both ecological function  
135 and human/livestock supply, and most of the rural residents in the SNW rely on groundwater for domestic and farm  
136 use.

137 The SNW is characterized by relatively wet temperate climate with ample amounts of snow in winter and warm  
138 summers. The annual average temperature is just over 5 C, with average summer highs reaching 26°C in July and  
139 average winter lows reaching -14°C in January ([https://climate.weather.gc.ca/climate\\_normals](https://climate.weather.gc.ca/climate_normals)). Present day  
140 landcover (Fig. 1) consists of 38% cropland, 29% forest, 20% grassland, 7% urban, 5% wetland, and 1% water. The  
141 dairy industry is a big part of the SNW economy, and the grassland areas provide grazing area to feed the cattle.



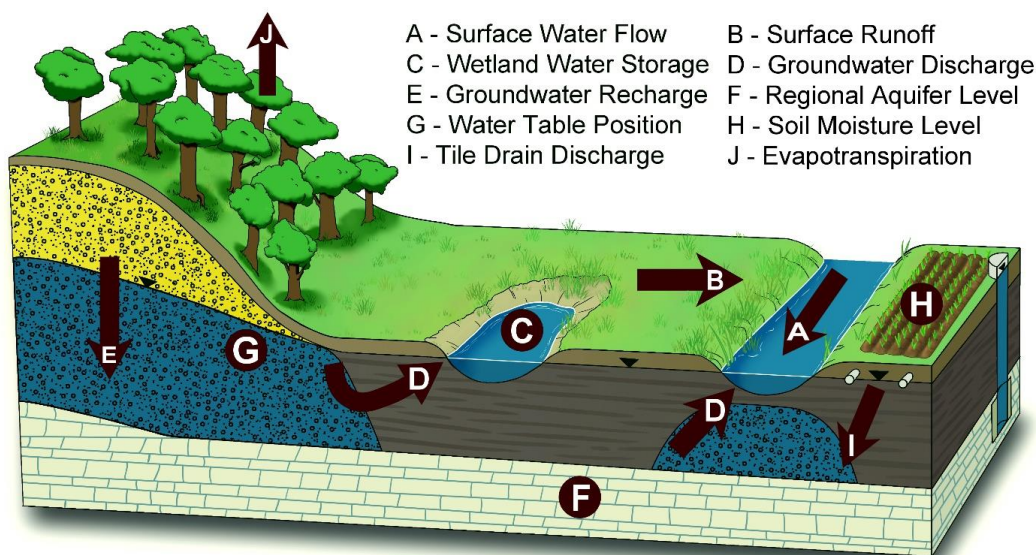
142

143 Figure 1: Location of the South Nation Watershed (SNW) in North America. The figure in the inset (right) shows the  
144 land use types in the SNW.

## 145 2.2 Capturing changes in water storages using HGS Model

146 As HGS is a fully integrated model, it generates simulation outputs for all components of the terrestrial hydrologic  
147 cycle (Fig. 2) in a completely transient format, thus alleviating a common limitation of ecosystem services models in  
148 that they do not account for transient behavior (Vigerstol and Aukema, 2011). Furthermore, HGS outputs can also be  
149 generated for the entire model domain (i.e., the watershed) or refined for smaller spatial scales such as subwatersheds,  
150 with the downscale limit being that of an individual finite element within the Finite Element Method (FEM).





151

152 Figure 2: Key components of terrestrial hydrological cycle mapped by the HGS model

153 However, it should be noted that the integrity of the HGS outputs are also dependent on the model scale, in that, for  
154 example, a model of a 150,000 km<sup>2</sup> river basin is best suited to answer big picture questions (i.e., basin water balance,  
155 climate change impacts, regional groundwater), while a model built for the SNW can be used to address questions  
156 pertaining to localized processes (i.e., individual wetland influences, groundwater recharge and discharge patterns,  
157 flood extent, local aquifer conditions, local soil moisture conditions). If even more localized insights are required,  
158 HGS models can be resolved down to field or plot scale, where highly detailed questions pertaining to things such as  
159 riparian zones, soil structure, manure application, and tile drainage influences on water quantity and quality can be  
160 evaluated. However, for field or plot scale insights, the model domain typically would be no larger than 10 – 20 km<sup>2</sup>.  
161 Thus, HGS is a scalable and robust model. We use the model to capture watershed surface water outflow, actual  
162 evapotranspiration (ET<sub>a</sub>) (which are correlated to biomass production), subsurface water storage, and land surface  
163 water storage (reflective of how much water is held in wetlands and reservoirs).

## 164 2.2.1 Model construction

### 165 2.2.1.1 Finite Element Mesh (FEM)

166 The HGS model utilizes a 3-D unstructured finite element mesh (FEM) that extends across the full 3830 km<sup>2</sup> area of  
167 the SNW. Within the structure of the FEM are 1-D river/stream channel features, a 2-D overland flow domain

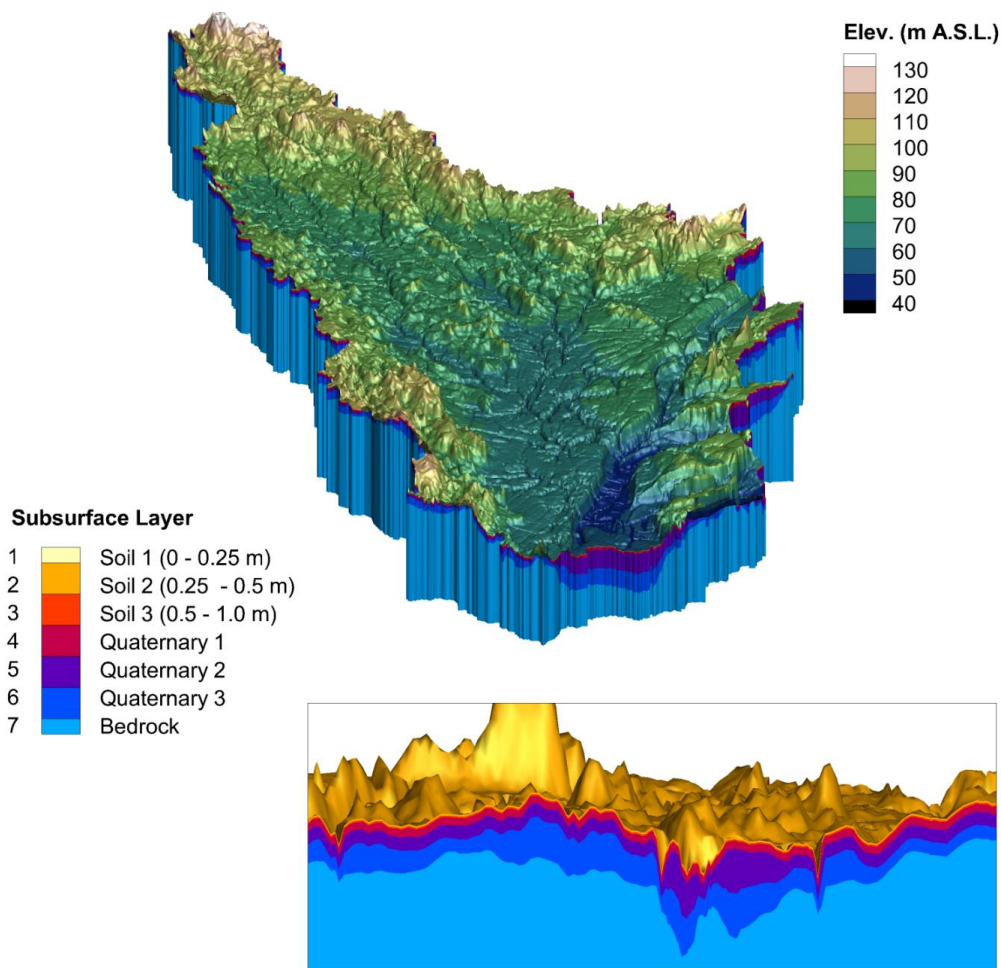


168 (reflecting land surface topography), and a 3-D subsurface flow domain (reflecting hydrostratigraphy). The FEM for  
169 the SNW model resolves all Strahler 2+ stream/river features as control lines in the mesh. FEM node spacing (element  
170 edge length) was maintained at 100 m along the control lines, while away from the control lines the node spacing  
171 extends up to 300 m. On each FEM layer there is a total of 86,740 nodes and 171,609 finite elements. Accordingly,  
172 over the eight subsurface mesh sheets (seven subsurface layers); the FEM contains 693,920 nodes and 1,201,263 3-D  
173 finite elements. In addition, the surface layer contains an additional 86,740 nodes and 171,609 2-D finite elements.

#### 174 **2.2.1.2 Hydrostratigraphy**

175 The seven subsurface layers represent (from the top down) three soil layers, three Quaternary geology layers, and one  
176 bedrock layer. The soil layers extend from 0–0.25 m, 0.25–0.5 m, and 0.5–1 m depth relative to the top surface, which  
177 is defined using the Ontario Integrated Hydrology digital elevation model (Ontario Integrated Hydrology Data:  
178 Elevation and mapped water features for provincial scale hydrology applications). The hydraulic properties for the  
179 soil layers vary spatially according to the soil polygons defined in the Soil Landscapes of Canada (SLC, Soil  
180 Landscapes of Canada Working Group, 2010), and are defined in two steps as follows: (1) properties extracted from  
181 SLC are used in conjunction with the Rosetta pedotransfer functions (Schaap et al., 2001) to obtain estimates for  
182 hydraulic conductivity, water retention and relative permeability, residual saturation, and porosity parameters, and (2)  
183 hydraulic conductivity, water retention and relative permeability parameters are manually tuned during model  
184 calibration. The three Quaternary layers are of variable thickness, where the layer interfaces represent contrasting  
185 lithology using a simplified version of the 3-D geological model produced by Logan et al., (2009). Hydraulic  
186 properties for the Quaternary materials are assigned based on lithology. Underlying the Quaternary layers is a single  
187 layer of uniform hydraulic conductivity representative of the Phanerozoic bedrock. When assembled, the model layers  
188 depict a 3-D subsurface realization of the SNW hydrostratigraphy (Fig. 3).





189

190 Figure 3: Three-dimensional perspective of the South Nation HydroGeoSphere model, and the hydrostratigraphic  
191 layering (inset). Note the 100x vertical exaggeration.

### 192 2.2.1.3 Land Surface Configuration

193 The land surface in the HGS model represents land cover distribution defined by the gridded, 30 m resolution, 2017  
194 Annual Crop Inventory dataset (Annual Space-Based Crop Inventory for Canada, 2017), that is refined to six  
195 categories (water, urban, wetland, grassland, cropland, and forest). Root depth for the cropland (1 m), forest (2.9 m),  
196 wetland (1 m), grassland (2.1 m), and urban (1 m) landcovers was held static over the simulation interval. Spatially  
197 distributed leaf area index (LAI) is a transient parameter represented by the 8-day composite, 500 m resolution  
198 MOD15A2H v006 data product (MYD15A2H MODIS/Aqua Leaf Area Index/FPAR 8-Day L4 Global 500m SIN



199 Grid. NASA LP DAAC). Each landcover category also utilized a unique value for surface roughness (Manning's  $n$   
200 coefficient), ranging from 0.001 (urban) to 0.03  $\text{s/m}^{1/3}$  (forest).

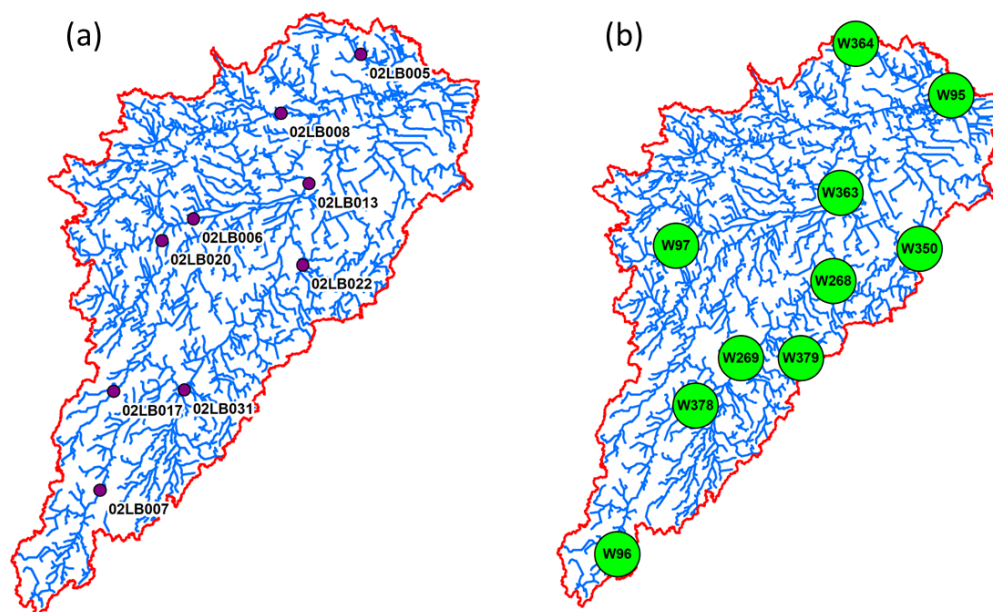
#### 201 **2.2.1.4 Climatology**

202 Time-varying and spatially distributed climate data with daily temporal resolution is used as forcing for the liquid  
203 water influx (LWF) and potential evapotranspiration (PET) boundary conditions in the HGS model for the 2000 to  
204 2018 simulation interval. LWF is derived from precipitation obtained from McKenney et al. (2011) in combination  
205 with snow water equivalent (SWE) estimates from the ERA5-Land land-surface reanalysis (Muñoz-Sabater et al.,  
206 2021), where LWF is the sum of liquid precipitation (rain) and snowmelt (daily changes in SWE).

207 Potential evapotranspiration (PET) is used to calculate  $ET_a$  within HGS. PET primarily depends on the surface  
208 radiation budget, temperature, humidity, and near-surface wind speed (Allen et al., 1998); however, out of these  
209 variables, only minimum and maximum temperature are readily available for the full SNW. Hence, PET forcing for  
210 the SNW model is calculated with the Hogg method (Hogg, 1997). This is consistent with Erler et al. (2019) and Xu  
211 et al. (2021), who reported good agreement with the observed water balance in the Great Lakes region when using the  
212 Hogg method. The Hogg method is based on the FAO Penman-Monteith approach (Allen et al. 1998), where the  
213 radiation budget and humidity are approximated as a function of daily minimum and maximum temperature (and wind  
214 is assumed to be constant).

#### 215 **2.2.2 Model Performance Evaluation**

216 The performance of the SNW HGS model is evaluated using observed surface water flow rates and groundwater levels  
217 from across the watershed. The observation data is derived from surface water flow monitoring conducted at 9 Water  
218 Survey of Canada (WSC) hydrometric stations (Figure 4a) and 10 Provincial Groundwater Monitoring Network wells  
219 (Figure 4b). The Nash-Sutcliffe Efficiency (NSE) and Percent Bias (Pbias) metrics (Moriassi et al., 2007) are used to  
220 evaluate surface water flow simulation performance, while the coefficient of determination ( $R^2$ ) is used to evaluate  
221 groundwater simulation performance.



222

223 Figure 4. Distribution of (a) Water Survey of Canada surface water flow gauges, and (b) Provincial Groundwater  
224 Monitoring Network wells across the South Nation watershed.

### 225 2.3 Ecosystem services water productivity

226 We use the benefit transfer method to derive the unit values of ecosystems in the SNW. The value transfer method,  
227 which is a widely used and quick technique for assessing the economic value of ecosystem services, relies on  
228 secondary data obtained through the implementation of various other economic valuation methods (Aziz, 2021). A  
229 local study by L'Ecuyer-Sauvageau et al. (2021) assembles the values for 13 ecosystem services: agricultural services,  
230 global climate regulation, air quality, water provision, waste treatment, erosion control, pollination, habitat for  
231 biodiversity, natural hazard prevention, pest management, nutrient cycling, landscape aesthetics, and recreational  
232 activities. Because of unavailability of data, raw material, genetic diversity, spiritual, cultural and heritage identity  
233 services are excluded from the analysis. These unit values have been correspondingly generated by major ecosystems  
234 in the adjacent Ottawa-Gatineau region using market price, replacement cost, and benefit transfer methods. The unit  
235 values for ecosystem services are gathered based on similarities of ecologic and socio-economic conditions between  
236 the studied and policy sites, and converted using the purchasing power parity (L'Ecuyer-Sauvageau et al., 2021). After



237 adjusting these values for inflation, we calculate the value of ecosystem services in the SNW for the simulation period  
238 using the following equation.

$$239 \quad EV_t = \sum_{k=1}^n (A_k \times UV_k) * VI \quad (1)$$

240  $A_k$ = Area of land use  $k$

241  $UV_k$ = Unit value of ecosystem services for land use  $k$

242  $VI$ = Vegetation indicator, a ratio of yearly to average net primary production= $NPP_{year}/NPP_{mean}$

243 We use net primary production as an indicator to characterize the vegetation vigor (Xu et al., 2012) and to adjust the  
244 values of ecosystem services over time in the SNW. The relative vegetation indicator (VI) is the ratio of yearly NPP  
245 and the mean NPP over the selected period. The Moderate Resolution Imaging Spectroradiometer (MODIS) data  
246 (<https://appears.earthdatacloud.nasa.gov/>) for NPP (at 500m resolution) is collected from 2000 to 2017. Using the  
247 spatial analyst tool of ArcGIS and raster data for NPP, we calculate yearly mean values of NPP over the selected time  
248 period. The average NPP values from 2000-2017 for the SNW are given in Table 1.

249 We then calculate the average ecosystem services water productivity using ecosystem services values and green water  
250 volumes in equation 2:

$$251 \quad V_w = (EV_t)/(X_w) \quad (2)$$

252  $V_w$  is the average product of water (\$ per  $m^3$ ),  $X_w$  is the total volume of  $ET_a$ /green water used in a year 't'.

#### 253 **2.4 Valuation of subsurface water contribution towards ecosystem services supply**

254 Firstly, we develop a water production function for ecosystem services supply using total values of the watershed over  
255 the 18-year period and corresponding volumes of green water consumed. Because ecosystem services value is  
256 proportional to biomass production (Costanza et al., 1998), the values are modified over the time using relative  
257 changes in biomass of ecosystems in the watershed (Xu and Xiao, 2022). The slope of the production function  
258 represents the ecosystem services marginal water productivity ( $MP_w$ ). Secondly, the HGS model captures the volumes  
259 of subsurface and surface water used in supporting  $ET_a$ . Using the volumes of storages consumed for  $ET_a$  and  $MP_w$ ,  
260 the economic value of storages is calculated for ecosystem services supply (Eq.3).

$$261 \quad V_i = X_{wi} * MP_w \quad (3)$$

262 Where  $V_i$  is the value of water storage  $i$  towards ecosystem services supply,  $X_{wi}$  is the volume of water storage  $i$  used  
263 towards green water supply,  $MP_w$  is the marginal productivity of water.

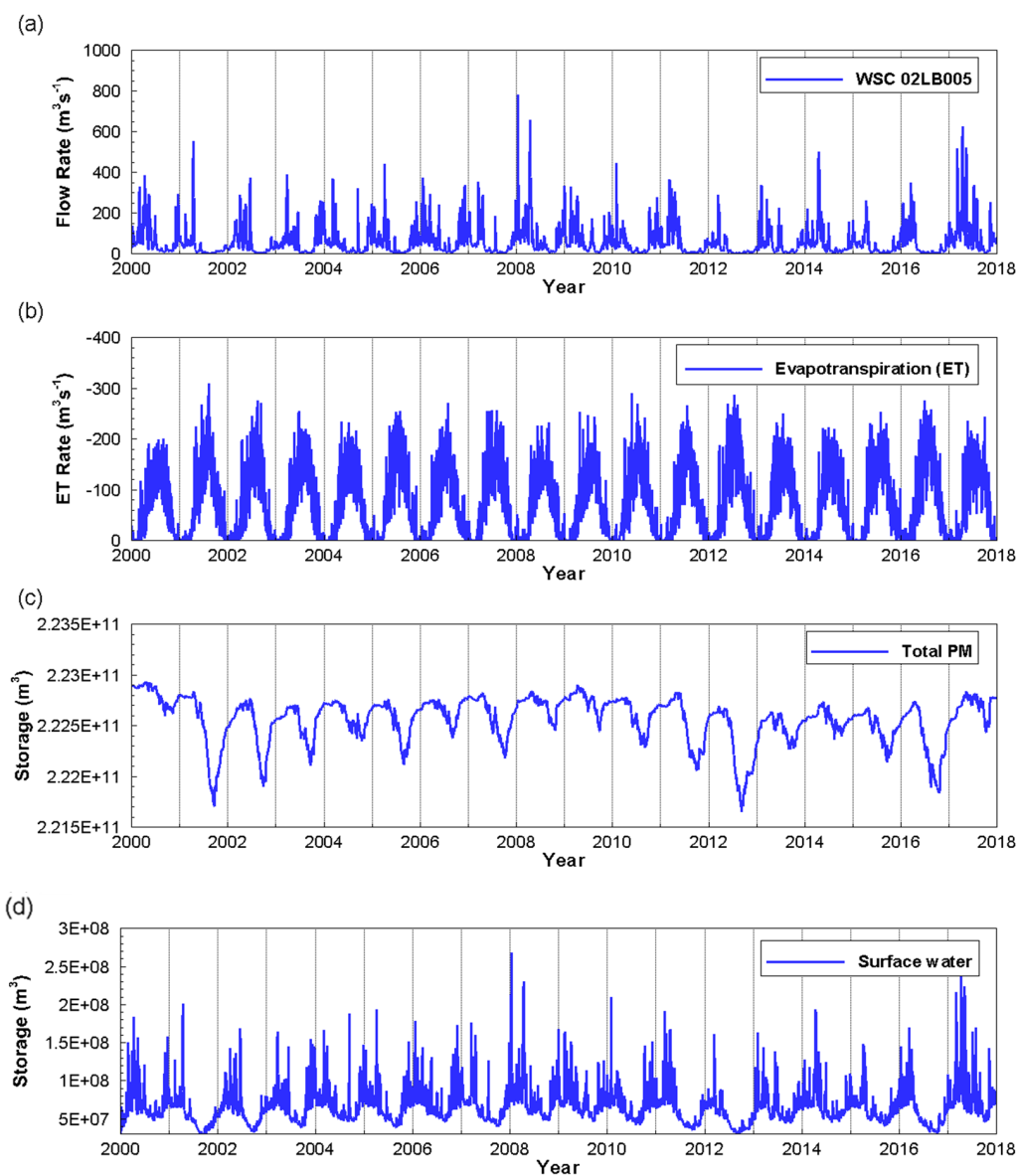


264 **3 Results**

265 **3.1 HGS outputs**

266 For the 2000 to 2018 simulation interval, the HGS model is able to reproduce surface water flow rates at the nine  
267 WSC hydrometric stations across the SNW with good accuracy. Based on daily evaluation frequency, NSE ranged  
268 from 0.59 to 0.70, with a mean of 0.66; while PBias ranged from -17.4 % to 17.1 %, with a mean of 3.9 %. Groundwater  
269 levels were also reproduced across the SNW with reasonable accuracy for the 2000 to 2018 interval. The  $R^2$  between  
270 simulated and observed water levels in the 10 observation wells is 0.98, with the simulated values having a mean value  
271 2.8 m higher than the observed values.

272 HGS outputs (Fig. 5) represent conditions associated with continuous simulation of the SNW over 2000 to 2017 time  
273 interval, and the calibration metrics are also based over the same time interval. Included are watershed surface water  
274 outflow,  $ET_a$  rates (which are correlated to biomass production), subsurface water storage (groundwater storage plus  
275 soil moisture storage) and land surface water storage. These storage zones recharge and discharge over time, but the  
276 biggest dip is shown in 2012—the drought year.



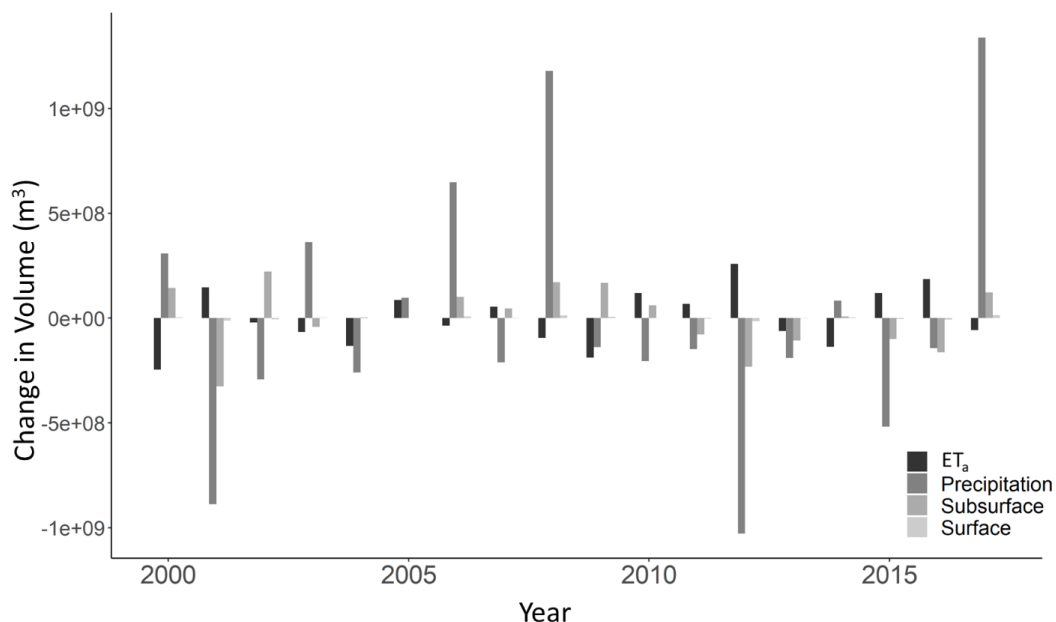
277

278 Figure 5: Time series outputs from the South Nation watershed HydroGeoSphere (HGS) simulation over the 2003-to-  
279 2018-time interval. (a) stream flow at a representative gauge location, (b) watershed evapotranspiration, (c) watershed  
280 subsurface water storage, and (d) watershed land surface water storage.

281 We aggregate the daily values to yearly values to counter the lag affects. The numeric data for the variables presented  
282 in Fig. 5 is given in the Table 1A. The mean change is calculated to analyze the fluctuations in the storages over time



283 (Fig. 6). The year 2012 (the drought year) shows the maximum increase in evapotranspiration and a high dip in the  
 284 subsurface water storage.



285

286 Figure 6: Mean changes in surface and subsurface water storages, ET<sub>a</sub>, and precipitation over time

287 **3.2 Valuation of ecosystem services, and average and marginal water productivity**

288 The unit values developed for major land use types in the SNW are given in table 1

289 Table 1: Land use types and unit values for the SNW

Land Use	Area (hectare)	Unit value (\$/hectare/year)
Water	1,299	165
Urban	25,734	1,177
Wetlands	16,709	71,273
Native Grasslands	7,6961	4,152
Croplands	154,810	1,666
Forest	107,470	4,993

290



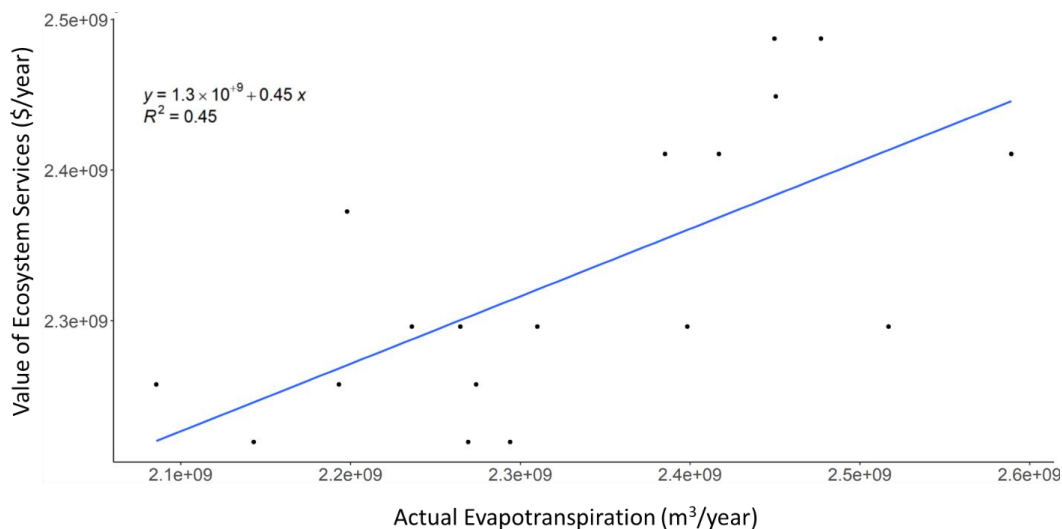


291 Using the unit values (Table 1) and land use area, we calculate a total value of \$2.33 billion per year for 13 ecosystem  
 292 services in the SNW and the value is further modified for each year using the NPP values in Eq. 2. The estimates for  
 293 average product of water are point estimates for each year based on the value of ecosystem services and green water  
 294 volume for the corresponding year. The NPP data, ES values,  $ET_a$  and average water product in the SNW for each  
 295 year are given in the Table 2.

296 Table 2: Mean NPP, ecosystem services (ES) values and average water product for the SNW from 2000 to 2017

Year	Mean NPP (Kg C/m <sup>2</sup> /year)	ES Value (x10 <sup>9</sup> \$/year)	$ET_a$ (x10 <sup>9</sup> m <sup>3</sup> )	Average product of water (\$/m <sup>3</sup> )
2000	0.59	2.26	2.09	1.08
2001	0.65	2.49	2.48	1.00
2002	0.6	2.30	2.31	0.99
2003	0.6	2.30	2.26	1.01
2004	0.62	2.37	2.20	1.08
2005	0.63	2.41	2.42	1.00
2006	0.58	2.22	2.29	0.97
2007	0.63	2.41	2.39	1.01
2008	0.6	2.30	2.24	1.03
2009	0.58	2.22	2.14	1.04
2010	0.64	2.45	2.45	1.00
2011	0.6	2.30	2.40	0.96
2012	0.63	2.41	2.59	0.93
2013	0.58	2.22	2.27	0.98
2014	0.59	2.26	2.19	1.03
2015	0.65	2.49	2.45	1.02
2016	0.6	2.30	2.52	0.91
2017	0.59	2.26	2.27	0.99

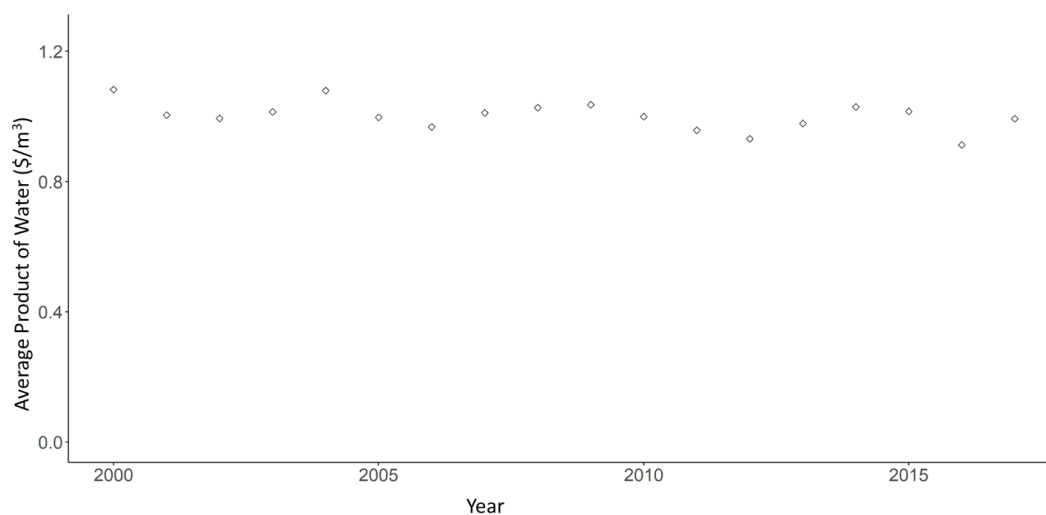
297 For the ecosystem services marginal water productivity, we develop a production function using  $ET_a$  and ES values  
 298 for the SNW (Fig. 7). The slope of the production function is marginal productivity of water, which is \$0.45/m<sup>3</sup> in the  
 299 SNW.



300

301 Figure 7: Ecosystem services water production function in the SNW

302 To assess the contribution of subsurface water towards ecosystem services, we calculate the average ecosystem  
303 services water productivity at the watershed scale. The average product of water over the modeling period of 18 years  
304 ranges from \$0.91-1.08 per m<sup>3</sup> (Fig. 8). During the drought periods (years 2001, 2012 and 2016), the average product  
305 of water declines and is minimum. The average product shows efficiency in use of water across the modeling period.  
306 It is the maximum for year 2000, meaning the conditions (other variables like precipitation) were favoring the  
307 maximum production of ecosystem services with the lowest water consumption in that year.

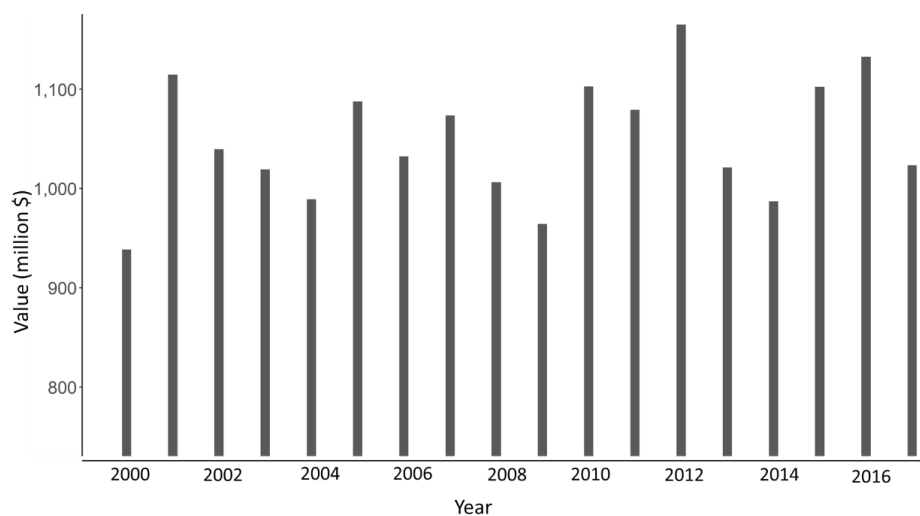


308

309 Figure 8: Average product of water for ecosystem services in the SNW

### 310 3.3 Valuation of green, subsurface, and surface waters

311 Using the marginal water productivity and  $ET_a$  in the SNW, we calculate the value of green water over the modelling  
312 period (Fig. 9).

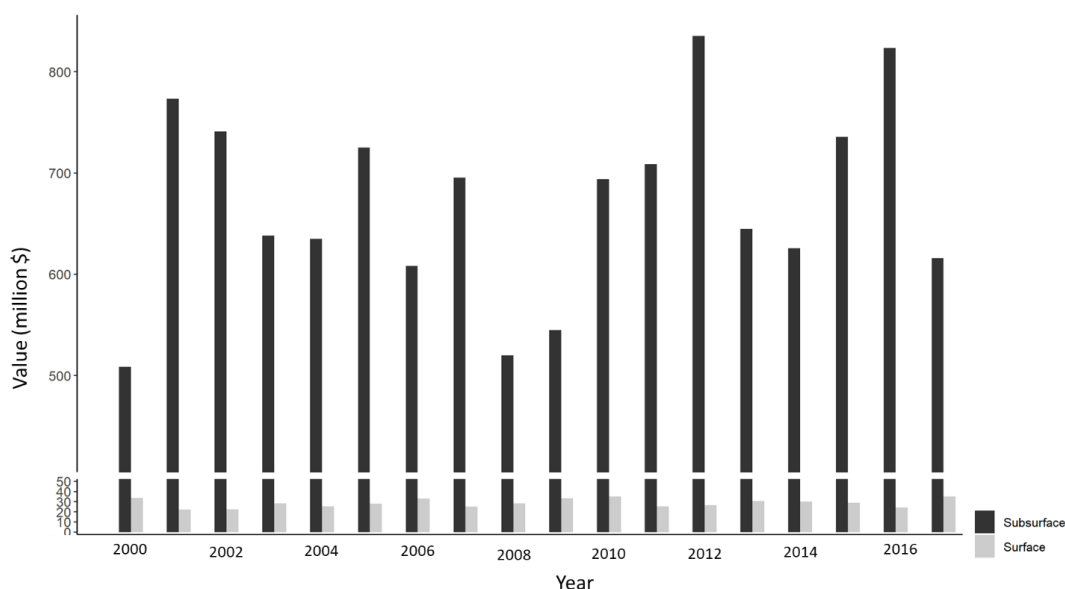


313

314 Figure 9: Value of green water in the SNW



315 We use the subsurface water evapotranspiration and surface water evaporation to calculate the contribution of these  
316 two storages towards  $ET_a$ . Finally, these contributions in terms of water volume are valued using the marginal value  
317 of water to account for subsurface and surface water inputs to the green water supply.



318

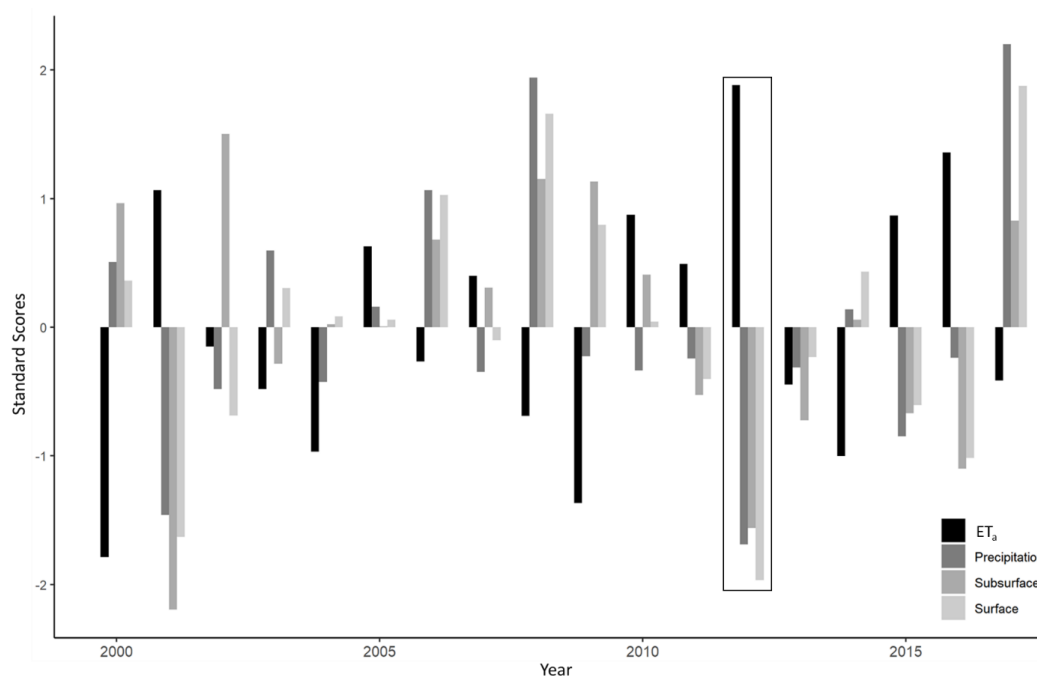
319 Figure 10: Contribution of subsurface and surface water towards green water supply in the SNW. (Note the break in  
320 y-axis from 50 to 500)

#### 321 4 Discussion

322  $ET_a$  is a key phenomenon that sustains terrestrial ecosystem functions such as biomass production, and thus helps to  
323 supply a variety of ecosystem services. As a fully integrated model, HGS generates simulation outputs for all  
324 components of the terrestrial hydrologic cycle in a completely transient format, thus alleviating a common limitation  
325 of most water models in that they do not account for transient behavior (Vigerstol and Aukema, 2011). We use HGS  
326 to capture fluctuations in subsurface water and surface water storages, which can be used to quantify the role of these  
327 storages in sustaining  $ET_a$  and subsequent ecosystem services. Then we compute the change in these zones with respect  
328 to mean storage. Our modelling results show that  $ET_a$  is mainly supported by subsurface water storage/fluctuations  
329 with respect to magnitude/quantity of water consumed.



330 To further compare the fluctuations in different storage zones on a common scale, we compute the standard scores  
331 (that is, the change in a storage/standard deviation) for each zone over time (Fig. 11). The standard scores show that  
332  $ET_a$  is supported by both surface and subsurface water storages during the drought periods. However, the contribution  
333 of subsurface water by volume during dry periods is much bigger than that of surface water. That is, the subsurface  
334 water shores up the surface water during droughts.



335  
336 Figure 11: Change in standard scores of water storages/hydrological variables over the modeling period. The scores  
337 for an anomaly year (2012) are bordered.

338 The comparison of years 2001 and 2012 (with less precipitation than mean) shows that the  $ET_a$  was less but outflow  
339 was more in year 2001 than in 2012 (Fig. 5(a)). Thus, the drawdown in subsurface water in 2001 maintained the flows  
340 in water bodies and streams in the watershed. The different response of subsurface water to two droughts (in years  
341 2001 and 2012) in the watershed depends on the amounts of precipitation and other climatic conditions (e.g.,  
342 temperature, atmospheric moisture demand, etc.) in the corresponding years (Zhao et al., 2022). During drought  
343 periods, water demand for  $ET_a$  increases in most parts of the world due to high atmospheric moisture demand, resulting  
344 in ecosystem stress and depletion of (subsurface and surface) water storages (Zhao et al., 2022). Similar to worldwide  
345 trends described in Zhao et al. (2022), the  $ET_a$  rates in our study increase during dry periods. Given the complexities



346 involved in linking  $ET_a$  with surface and subsurface water storages, the impact of variations in  $ET_a$  rates on ecosystem  
347 services during droughts remains unknown.

348 Our study is seminal in capturing the ecosystem services values with changing water supply/balance in a watershed  
349 over a period of time. Few studies in the literature (e.g., Loheide, 2008; Su et al., 2022) have only estimated  
350 groundwater evapotranspiration by linking water table fluctuation and changes in evapotranspiration. However, given  
351 the flow of groundwater to soil vadose zone and surface water bodies, this approach of using water table fluctuations  
352 is unable to yield accurate estimation of groundwater contribution towards sustaining evapotranspiration. The more  
353 sophisticated HGS approach, by computing the subsurface water evaporation and transpiration, and surface water  
354 evaporation, can assess the connections between  $ET_a$  and water storages more robustly.

355 The fluctuations in storages show that, in general, subsurface water storage repletes when  $ET_a$  is negative and depletes  
356 when  $ET_a$  is positive. The years 2001 and 2012, drought years, are anomalies:  $ET_a$  is relatively higher than during the  
357 wet years (high precipitation). The  $ET_a$  in drought years was mainly supported by the drawdown (by volume) in the  
358 subsurface water storage below the mean level. Fluctuations in the subsurface water storage across the 18 years are  
359 consistent with the changes in the precipitation, that is with above-average precipitation, the subsurface water storage  
360 increases and vice-versa. On the other hand, increase in  $ET_a$  leads to reduction in subsurface storage and vice-versa.

361 The maximum recharge in the subsurface water storage occurs in the year 2002, immediately following a 2001 severe  
362 dry period (within a 100-year time span) (Wheaton et al., 2008); 2002 was a year with less than average precipitation.

363 In regards to the economic valuation of water components, green water mainly benefits people at local scales (by  
364 supporting biomass and ecosystem services in the area) whereas the benefits of blue water are seen at a wider basin  
365 scale (Falkenmark and Rockström, 2010). Incorporating green-blue water resources at a watershed scale helps  
366 integrate the role of water in land use and other terrestrial ecosystem functions. Therefore, for better management of  
367 regional water resources, the use of fine-grained models becomes imperative to value the contributions of major  
368 inland water storages towards green water supply. We develop a water production function using total green water  
369 volumes and total values of SNW for 13 ecosystem services: agricultural services (net benefits from the crops or  
370 agricultural products), global climate regulation, air quality, water provision, waste treatment, erosion control,  
371 pollination, habitat for biodiversity, natural hazard prevention, pest management, nutrient cycling, landscape  
372 aesthetics, and recreational activities. The ecosystem water production function yields a marginal value of \$ 0.45 per  
373  $m^3$  of green water/  $ET_a$  (Fig. 7). Globally, Lowe et al. (2022) estimated the average marginal product of water at



374 \$0.083 per m<sup>3</sup> for crop production only. Additional ET<sub>a</sub> supplies ecosystem services at a constant rate; however,  
375 because the linear segment has a positive vertical intercept, the average ecosystem services water productivity  
376 decreases with increase in ET<sub>a</sub> as the slope of the ray from origin through a point on production function diminishes  
377 (Wichelns, 2014). On one hand, the water productivity will be maximum at the smallest amount of water  
378 used/consumed but, on the other hand, it will also produce the smallest value of ecosystem services in the watershed.  
379 Higher amounts of water are evapotranspired in the drought years mainly due to drought-associated meteorological  
380 conditions such as increase in temperatures (Zhao et al., 2022). However, NPP does not reduce during the drought  
381 periods, a finding consistent with other studies on temperate watersheds (e.g., Hosen et al., 2019; Sun et al., 2016).  
382 Our results show that the drought-induced water stress increases the ET<sub>a</sub> rates in the watershed, similar to Zhao et al.  
383 (2022) and Diao et al. (2021). The increase in ET<sub>a</sub> associated with a little higher of NPP for drought years across the  
384 modeling period lowers the ecosystem services water productivity during the dry periods in the watershed (Fig. 8).  
385 In the SNW, more of green water is used during the dry years with less precipitation. Therefore, the green water has  
386 a maximum value of \$1,165 million for year 2012—a drought year (Fig. 9). In this value, the subsurface and surface  
387 water contributions are \$835.6 and \$26.5 million, respectively (Fig. 10). The maximum contribution of the subsurface  
388 water is also for the year 2012 and then in 2001, both drought years. Contrarily, the surface water contributes a  
389 maximum of \$35.2 million in year 2010—a relatively wet year. Because surface water availability declines during  
390 droughts, its contribution towards green water supply diminishes. Over the 18-year modeling period in the SNW, the  
391 subsurface water contribution towards green water supply varies from 52% to 73%, whereas surface water contribution  
392 ranges from 2% to 3.6%. One reason that further adds to reduction in the surface contribution may be the tile drainage  
393 in the watershed (Miller and Lyon, 2021). Nonetheless, the critical role that the subsurface water provides in sustaining  
394 ecosystem services during dry periods in the watershed is evident.

395 Our methodology provides a basis for setting up a new model to assess the subsurface water contribution in other  
396 places. The results and values used in the study are not transferable to other sites/watersheds. The marginal product  
397 of water is a site-specific entity which will be different for other watersheds because both ecosystem services value  
398 and ET<sub>a</sub> will change depending on land cover (mainly), NPP, precipitation, and soil types. Nevertheless, given the  
399 dynamicity of the storages and their link to terrestrial ecosystem services, this valuation approach will yield reliable  
400 results provided the entire methodology (modelling of water storages and ET<sub>a</sub>, and valuation of ecosystem services)  
401 is conducted accurately for other locations/sites/watersheds.





402 **5 Conclusions**

403 Subsurface water plays a key role in the supply of terrestrial ecosystem services. Until now, subsurface water has  
404 never been comprehensively valued for its contribution towards ecosystem services supply in a watershed. The  
405 primary impediment has been complexities involved in modeling of interdependencies in hydrologic fluxes such as  
406 connection between subsurface water discharge and green water use. Despite known connectivity, subsurface, land  
407 and atmosphere water storages were modeled independently prior to the introduction of fully integrated hydrologic  
408 models. In our work in the SNW, we take the innovative approach of using the HGS model and ecosystem services  
409 valuation technique to monetize the contributions of surface and subsurface waters to the green water supply over a  
410 period of 18 years (2000-2017). The results show that droughts are a major trigger to increase the green water use in  
411 the watershed. At the same time, a bigger portion of the green water is supplied by the subsurface water, ranging from  
412 52% to 73% over the modeling period. The maximum green water value corresponded to year 2012 with severe  
413 drought conditions and equals \$1,165 million. More importantly, 72% of the green water value during the drought  
414 comes from the subsurface water contribution. Similarly, in other dry periods, years 2001 and 2016, the subsurface  
415 contribution makes 69% and 73% of the total green water values, respectively. Thus, the subsurface water plays a key  
416 role in supplying green water and sustaining ecosystem services during critical periods in the watershed. This analysis  
417 can help in better managing and allocating the subsurface water resources under climate uncertainties at a watershed  
418 scale.

419 **Author contribution**

420 Tariq Aziz contributed to the project by developing the concept, methodology, formal analysis, investigation, and  
421 writing the original draft.

422 Steven K. Frey was involved in conceptualization, methodology, data curation, HGS modeling, project administration,  
423 and reviewing and editing the manuscript.

424 David R. Lapen contributed to the project by helping develop the methodology, reviewing and editing the manuscript,  
425 and assisting with project administration.

426 Susan Preston assisted with reviewing and editing the manuscript and project administration.

427 Hazen A. J. Russell was responsible for reviewing and editing the manuscript.

428 Omar Khader contributed to the project by working on HGS modeling.

429 Andre R. Erler was involved in data curation and reviewing the manuscript.

430 Edward A. Sudicky was responsible for project administration and reviewing the manuscript.



431 **Declaration of interest**

432 The authors declare that they have no known competing financial interests or personal relationships that could have  
433 appeared to influence the work reported in this paper.

434 **References**

- 435 Annual Space-Based Crop Inventory for Canada, 2017: [https://open.canada.ca/data/en/dataset/32546f7b-55c2-481e-](https://open.canada.ca/data/en/dataset/32546f7b-55c2-481e-b300-83fc16054b95)  
436 [b300-83fc16054b95](https://open.canada.ca/data/en/dataset/32546f7b-55c2-481e-b300-83fc16054b95).
- 437 Allen, R. G., Pereira, L. S., Raes, D., and Smith, M.: Crop evapotranspiration guidelines for computing crop  
438 requirements, 1998.
- 439 An, S. and Verhoeven, J. T. A.: Wetlands: Ecosystem services, restoration and wise use, 325 pp., 2019.
- 440 Aziz, T.: Changes in land use and ecosystem services values in Pakistan, 1950–2050, *Environ. Dev.*, 35, 1,  
441 <https://doi.org/10.1016/j.envdev.2020.100576>, 2021.
- 442 Booth, E. G., Zipper, S. C., Loheide, S. P., and Kucharik, C. J.: Is groundwater recharge always serving us well?  
443 Water supply provisioning, crop production, and flood attenuation in conflict in Wisconsin, USA, *Ecosyst. Serv.*, 21,  
444 153–165, 2016.
- 445 Chen, X. and Hu, Q.: Groundwater influences on soil moisture and surface evaporation, *J. Hydrol.*, 297, 285–300,  
446 <https://doi.org/10.1016/j.jhydrol.2004.04.019>, 2004.
- 447 Clark, M. P., Fan, Y., Lawrence, D. M., Adam, J. C., Bolster, D., Gochis, D. J., Hooper, R. P., Kumar, M., Leung, L.  
448 R., Mackay, D. S., and Maxwell, R. M.: Hydrological partitioning in the critical zone: Recent advances and  
449 opportunities for developing transferable understanding of water cycle dynamics, *Water Resour. Res.*, 1–28,  
450 <https://doi.org/10.1002/2015WR017096>.Received, 2015.
- 451 Condon, L. E., Atchley, A. L., and Maxwell, R. M.: Evapotranspiration depletes groundwater under warming over the  
452 contiguous United States, *Nat. Commun.*, 11, <https://doi.org/10.1038/s41467-020-14688-0>, 2020.
- 453 Costanza, R., D’Arge, R., De Groot, R., Farber, S., Grasso, M., Hannon, B., Limburg, K., Naeem, S., O’Neill, R. V.,  
454 Paruelo, J., Raskin, R. G., Sutton, P., and Van Den Belt, M.: The value of ecosystem services: Putting the issues in  
455 perspective, *Ecol. Econ.*, 25, 67–72, [https://doi.org/10.1016/S0921-8009\(98\)00019-6](https://doi.org/10.1016/S0921-8009(98)00019-6), 1998.
- 456 Dennedy-Frank, P. J., Muenich, R. L., Chaubey, I., and Ziv, G.: Comparing two tools for ecosystem service  
457 assessments regarding water resources decisions, *J. Environ. Manage.*, 177, 331–340,  
458 <https://doi.org/10.1016/j.jenvman.2016.03.012>, 2016.
- 459 Diao, H., Wang, A., Yang, H., Yuan, F., Guan, D., and Wu, J.: Responses of evapotranspiration to droughts across  
460 global forests: A systematic assessment, *Can. J. For. Res.*, 51, 1–9, <https://doi.org/10.1139/cjfr-2019-0436>, 2021.
- 461 Erler, A. R., Frey, S. K., Khader, O., d’Orgeville, M., Park, Y. J., Hwang, H. T., Lapen, D. R., Richard Peltier, W.,  
462 and Sudicky, E. A.: Simulating Climate Change Impacts on Surface Water Resources Within a Lake-Affected Region  
463 Using Regional Climate Projections, *Water Resour. Res.*, 55, 130–155, <https://doi.org/10.1029/2018WR024381>,  
464 2019.
- 465 Falkenmark, M. and Rockström, J.: Building Water Resilience in the Face of Global Change: From a Blue-Only to a



- 466 Green-Blue Water Approach to Land-Water Management, *J. Water Resour. Plan. Manag.*, 136, 606–610,  
467 [https://doi.org/10.1061/\(asce\)wr.1943-5452.0000118](https://doi.org/10.1061/(asce)wr.1943-5452.0000118), 2010.
- 468 Foster, S. S. D. and Chilton, P. J.: Groundwater: The processes and global significance of aquifer degradation, *Philos.*  
469 *Trans. R. Soc. B Biol. Sci.*, 358, 1957–1972, <https://doi.org/10.1098/rstb.2003.1380>, 2003.
- 470 Griebler, C. and Avramov, M.: Groundwater ecosystem services: A review, *Freshw. Sci.*, 34, 355–367,  
471 <https://doi.org/10.1086/679903>, 2015.
- 472 Hogg, E. H.: Temporal scaling of moisture and the forest-grassland boundary in western Canada, *Agric. For.*  
473 *Meteorol.*, 84, 115–122, [https://doi.org/10.1016/S0168-1923\(96\)02380-5](https://doi.org/10.1016/S0168-1923(96)02380-5), 1997.
- 474 Honeck, E., Gallagher, L., von Arx, B., Lehmann, A., Wyler, N., Villarrubia, O., Guinaudeau, B., and Schlaepfer, M.  
475 A.: Integrating ecosystem services into policymaking – A case study on the use of boundary organizations, *Ecosyst.*  
476 *Serv.*, 49, <https://doi.org/10.1016/j.ecoser.2021.101286>, 2021.
- 477 Hosen, J. D., Aho, K. S., Appling, A. P., Creech, E. C., Fair, J. H., Hall, R. O., Kyzivat, E. D., Lowenthal, R. S., Matt,  
478 S., Morrison, J., Saiers, J. E., Shanley, J. B., Weber, L. C., Yoon, B., and Raymond, P. A.: Enhancement of primary  
479 production during drought in a temperate watershed is greater in larger rivers than headwater streams, *Limnol.*  
480 *Oceanogr.*, 64, 1458–1472, <https://doi.org/10.1002/lno.11127>, 2019.
- 481 Jin, Z., Liang, W., Yang, Y., Zhang, W., Yan, J., Chen, X., Li, S., and Mo, X.: Separating Vegetation Greening and  
482 Climate Change Controls on Evapotranspiration trend over the Loess Plateau, *Sci. Rep.*, 7, 1–15,  
483 <https://doi.org/10.1038/s41598-017-08477-x>, 2017.
- 484 L’Ecuyer-Sauvageau, C., Dupras, J., He, J., Auclair, J., Kermagoret, C., and Poder, T. G.: The economic value of  
485 Canada’s National Capital Green Network, *PLoS One*, 16, 1–29, <https://doi.org/10.1371/journal.pone.0245045>, 2021.
- 486 Li, Q., Qi, J., Xing, Z., Li, S., Jiang, Y., Danielescu, S., Zhu, H., Wei, X., and Meng, F. R.: An approach for assessing  
487 impact of land use and biophysical conditions across landscape on recharge rate and nitrogen loading of groundwater,  
488 *Agric. Ecosyst. Environ.*, 196, 114–124, <https://doi.org/10.1016/j.agee.2014.06.028>, 2014.
- 489 Liu, Y. and El-Kassaby, Y. A.: Evapotranspiration and favorable growing degree-days are key to tree height growth  
490 and ecosystem functioning: Meta-Analyses of Pacific Northwest historical data, 1st Annu. IEEE Conf. Control  
491 Technol. Appl. CCTA 2017, 2017-Janua, 7–12, <https://doi.org/10.1038/s41598-018-26681-1>, 2017.
- 492 Liu, Y., Zhou, R., Wen, Z., Khalifa, M., Zheng, C., Ren, H., Zhang, Z., and Wang, Z.: Assessing the impacts of  
493 drought on net primary productivity of global land biomes in different climate zones, *Ecol. Indic.*, 130, 108146,  
494 <https://doi.org/10.1016/j.ecolind.2021.108146>, 2021.
- 495 Logan, C., Cummings, D. I., Pullan, S., Pugin, A., Russell, H. A. J., and Sharpe, D. R.: Hydrostratigraphic model of  
496 the South Nation watershed region, south-eastern Ontario, Geological Survey of Canada, 17 pp.,  
497 <https://doi.org/https://doi.org/10.4095/248203>, 2009.
- 498 Loheide, S. P.: A method for estimating subdaily evapotranspiration of shallow groundwater using diurnal water table  
499 fluctuations, *Ecohydrology*, 1, 59–66, 2008.
- 500 Lowe, B. H., Zimmer, Y., and Oglethorpe, D. R.: Estimating the economic value of green water as an approach to  
501 foster the virtual green-water trade, *Ecol. Indic.*, 136, 108632, <https://doi.org/10.1016/j.ecolind.2022.108632>, 2022.
- 502 Mammola, S., Cardoso, P., Culver, D. C., Deharveng, L., Ferreira, R. L., Fišer, C., Galassi, D. M. P., Griebler, C.,



- 503 Halse, S., Humphreys, W. F., Isaia, M., Malard, F., Martinez, A., Moldovan, O. T., Niemiller, M. L., Pavlek, M.,  
504 Reboleira, A. S. P. S., Souza-Silva, M., Teeling, E. C., Wynne, J. J., and Zagamajster, M.: Scientists' warning on the  
505 conservation of subterranean ecosystems, *Bioscience*, 69, 641–650, <https://doi.org/10.1093/biosci/biz064>, 2019.
- 506 McKenney, D. W., Hutchings, M. F., Papadopol, P., Lawrence, K., Pedlar, J., Campbell, K., Milewska, E.,  
507 Hopkinson, R. F., Price, D., and Owen, T.: Customized spatial climate models for North America, *Bull. Am. Meteorol.*  
508 *Soc.*, 92, 1611–1622, <https://doi.org/10.1175/2011BAMS3132.1>, 2011.
- 509 Millenium Ecosystem Assessment (MEA): *Ecosystems and Human Well-Being: Synthesis*, Island Press, 285 pp.,  
510 <https://doi.org/10.1057/9780230625600>, 2005.
- 511 Miller, S. A. and Lyon, S. W.: Tile Drainage Increases Total Runoff and Phosphorus Export During Wet Years in the  
512 Western Lake Erie Basin, 3, 1–13, <https://doi.org/10.3389/frwa.2021.757106>, 2021.
- 513 Moriasi, D. N., Arnold, J. G., Van Liew, M. W., Bingner, R. L., Harmel, R. D., and Veith, T. L.: Model evaluation  
514 guidelines for systematic quantification of accuracy in watershed simulations, *Trans. ASABE*, 50, 885–900,  
515 <https://doi.org/10.13031/2013.23153>, 2007.
- 516 Muñoz-Sabater, J., Dutra, E., Agustí-Panareda, A., Albergel, C., Arduini, G., Balsamo, G., Boussetta, S., Choulga,  
517 M., Harrigan, S., Hersbach, H., Martens, B., Miralles, D. G., Piles, M., Rodríguez-Fernández, N. J., Zsoter, E.,  
518 Buontempo, C., and Thépaut, J. N.: ERA5-Land: A state-of-the-art global reanalysis dataset for land applications,  
519 *Earth Syst. Sci. Data*, 13, 4349–4383, <https://doi.org/10.5194/essd-13-4349-2021>, 2021.
- 520 MYD15A2H MODIS/Aqua Leaf Area Index/FPAR 8-Day L4 Global 500m SIN Grid. NASA LP DAAC:  
521 Neff, B. P., Day, S. M., Piggott, A. R., and Fuller, L. M.: Base flow in the Great Lakes basin, *U.S. Geol. Surv. Sci.*  
522 *Investig. Rep.*, 32, 2005.
- 523 Ochoa, V. and Urbina-Cardona, N.: Tools for spatially modeling ecosystem services: Publication trends, conceptual  
524 reflections and future challenges, *Ecosyst. Serv.*, 26, 155–169, <https://doi.org/10.1016/j.ecoser.2017.06.011>, 2017.
- 525 Ontario Geological Survey: *Surficial Geology of Southern Ontario*, Miscellaneous Release--Data 128-REV. Ontario  
526 Geological Survey., 1–7 pp., 2010.
- 527 Ontario Integrated Hydrology Data: Elevation and mapped water features for provincial scale hydrology applications:  
528 <https://geohub.lio.gov.on.ca/maps/mnrf::ontario-integrated-hydrology-oih-data/about>.
- 529 Qiu, J., Zipper, S. C., Motew, M., Booth, E. G., Kucharik, C. J., and Loheide, S. P.: Nonlinear groundwater influence  
530 on biophysical indicators of ecosystem services, *Nat. Sustain.*, 2, 475–483, [https://doi.org/10.1038/s41893-019-0278-](https://doi.org/10.1038/s41893-019-0278-2)  
531 [2](https://doi.org/10.1038/s41893-019-0278-2), 2019.
- 532 Richardson, M. and Kumar, P.: Critical Zone services as environmental assessment criteria in intensively managed  
533 landscapes, *Earth's Futur.*, 5, 617–632, <https://doi.org/10.1002/2016EF000517>, 2017.
- 534 Schaap, M. G., Leij, F. J., and Van Genuchten, M. T.: Rosetta: A computer program for estimating soil hydraulic  
535 parameters with hierarchical pedotransfer functions, *J. Hydrol.*, 251, 163–176, [https://doi.org/10.1016/S0022-](https://doi.org/10.1016/S0022-1694(01)00466-8)  
536 [1694\(01\)00466-8](https://doi.org/10.1016/S0022-1694(01)00466-8), 2001.
- 537 Schyns, J. F., Hoekstra, A. Y., Booij, M. J., Hogeboom, R. J., and Mekonnen, M. M.: Limits to the world's green  
538 water resources for food, feed, fiber, timber, and bioenergy, *Proc. Natl. Acad. Sci. U. S. A.*, 116, 4893–4898,  
539 <https://doi.org/10.1073/pnas.1817380116>, 2019.



- 540 Siebert, S., Burke, J., Faures, J. M., Frenken, K., Hoogeveen, J., Döll, P., and Portmann, F. T.: Groundwater use for  
541 irrigation - A global inventory, *Hydrol. Earth Syst. Sci.*, 14, 1863–1880, <https://doi.org/10.5194/hess-14-1863-2010>,  
542 2010.
- 543 SLC: Soil Landscapes of Canada Version 3.2, 2007–2008 pp., 2010.
- 544 Su, Y., Feng, Q., Zhu, G., Wang, Y., and Zhang, Q.: A New Method of Estimating Groundwater Evapotranspiration  
545 at Sub-Daily Scale Using Water Table Fluctuations, *Water (Switzerland)*, 14, 1–14,  
546 <https://doi.org/10.3390/w14060876>, 2022.
- 547 Sun, B., Zhao, H., and Wang, X.: Effects of drought on net primary productivity: Roles of temperature, drought  
548 intensity, and duration, *Chinese Geogr. Sci.*, 26, 270–282, <https://doi.org/10.1007/s11769-016-0804-3>, 2016.
- 549 Sun, G., Hallema, D., and Asbjornsen, H.: Ecohydrological processes and ecosystem services in the Anthropocene: a  
550 review, *Ecol. Process.*, 6, <https://doi.org/10.1186/s13717-017-0104-6>, 2017.
- 551 Tan, S., Wang, H., Prentice, I. C., and Yang, K.: Land-surface evapotranspiration derived from a first-principles  
552 primary production model, *Environ. Res. Lett.*, 16, <https://doi.org/10.1088/1748-9326/ac29eb>, 2021.
- 553 Taylor, R. G., Scanlon, B., Döll, P., Rodell, M., Van Beek, R., Wada, Y., Longuevergne, L., Leblanc, M., Famiglietti,  
554 J. S., Edmunds, M., Konikow, L., Green, T. R., Chen, J., Taniguchi, M., Bierkens, M. F. P., Macdonald, A., Fan, Y.,  
555 Maxwell, R. M., Yechieli, Y., Gurdak, J. J., Allen, D. M., Shamsudduha, M., Hiscock, K., Yeh, P. J. F., Holman, I.,  
556 and Treidel, H.: Ground water and climate change, *Nat. Clim. Chang.*, 3, 322–329,  
557 <https://doi.org/10.1038/nclimate1744>, 2013.
- 558 Vigerstol, K. L. and Aukema, J. E.: A comparison of tools for modeling freshwater ecosystem services, *J. Environ.*  
559 *Manage.*, 92, 2403–2409, <https://doi.org/10.1016/j.jenvman.2011.06.040>, 2011.
- 560 Wheaton, E., Kulshreshtha, S., Wittrock, V., and Koshida, G.: Dry times: Hard lessons from the Canadian drought of  
561 2001 and 2002, *Can. Geogr.*, 52, 241–262, <https://doi.org/10.1111/j.1541-0064.2008.00211.x>, 2008.
- 562 Wichelns, D.: Do estimates of water productivity enhance understanding of farm-level water management?, *Water*  
563 *(Switzerland)*, 6, 778–795, <https://doi.org/10.3390/w6040778>, 2014.
- 564 Xu, C., Li, Y., Hu, J., Yang, X., Sheng, S., and Liu, M.: Evaluating the difference between the normalized difference  
565 vegetation index and net primary productivity as the indicators of vegetation vigor assessment at landscape scale,  
566 *Environ. Monit. Assess.*, 184, 1275–1286, <https://doi.org/10.1007/s10661-011-2039-1>, 2012.
- 567 Xu, S., Frey, S. K., Erler, A. R., Khader, O., Berg, S. J., Hwang, H. T., Callaghan, M. V., Davison, J. H., and Sudicky,  
568 E. A.: Investigating groundwater-lake interactions in the Laurentian Great Lakes with a fully-integrated surface water-  
569 groundwater model, *J. Hydrol.*, 594, 125911, <https://doi.org/10.1016/j.jhydrol.2020.125911>, 2021.
- 570 Xu, Y. and Xiao, F.: Assessing Changes in the Value of Forest Ecosystem Services in Response to Climate Change  
571 in China, *Sustain.*, 14, <https://doi.org/10.3390/su14084773>, 2022.
- 572 Yang, H., Luo, P., Wang, J., Mou, C., Mo, L., Wang, Z., Fu, Y., Lin, H., Yang, Y., and Bhatta, L. D.: Ecosystem  
573 evapotranspiration as a response to climate and vegetation coverage changes in Northwest Yunnan, China, *PLoS One*,  
574 10, 1–17, <https://doi.org/10.1371/journal.pone.0134795>, 2015.
- 575 Yang, X. and Liu, J.: Assessment and valuation of groundwater ecosystem services: A case study of Handan City,  
576 China, *Water (Switzerland)*, 12, <https://doi.org/10.3390/w12051455>, 2020.



577 Zhao, M., Aa, G., Liu, Y., and Konings, A.: Evapotranspiration frequently increases during droughts, *Nat. Clim.*  
578 *Chang.*, 6904, 2022.

579 Zisopoulou, K., Zisopoulos, D., and Panagoulia, D.: Water Economics: An In-Depth Analysis of the Connection of  
580 Blue Water with Some Primary Level Aspects of Economic Theory I, *Water (Switzerland)*, 14,  
581 <https://doi.org/10.3390/w14010103>, 2022.

582

### 583 **Appendix**

584 The annual outputs ( $ET_a$ , surface water, subsurface water, precipitation and outflow) from the HGS model are given  
585 in Table 1A.



Table A1: HGS outputs from the SNW simulation

Year	ET <sub>a</sub> (m <sup>3</sup> )	Surface water (m <sup>3</sup> )	Subsurface water (m <sup>3</sup> )	Precipitati on (m <sup>3</sup> )	Outflo w (m <sup>3</sup> )	Surfac e evapor ation (m <sup>3</sup> )	Subsur face evapor ation (m <sup>3</sup> )	Subsurf ace transpir ation (m <sup>3</sup> )
2000	2,085,53 4,445	69,424,628	222,709,069,4 60	4,199,527, 096	76,327, 719	75,020, 473	184,37 4,990	945,999, 818
2001	2,477,00 4,097	54,513,422	222,240,461,9 50	3,003,497, 233	32,382, 847	49,049, 150	193,68 4,126	1,525,26 3,969
2002	2,309,98 4,877	61,588,887	222,788,771,4 12	3,598,706, 939	50,743, 315	49,496, 381	137,24 6,184	150,943 1,700
2003	2,264,69 6,091	68,998,342	222,524,086,3 05	4,253,877, 105	64,623, 628	63,041, 934	155,34 5,628	1,263,07 3,935
2004	2,197,97 4,479	67,358,376	222,569,571,6 66	3,631,932, 688	47,291, 949	56,472, 059	186,21 7,551	1,224,54 5,264
2005	2,416,95 8,064	67,153,617	222,566,818,8 92	3,988,298, 138	48,434, 304	62,293, 999	203,74 5,742	1407,71 8,083
2006	2,293,95 0,204	74,422,486	222,666,754,3 61	4,538,849, 536	77,813, 027	73,310, 604	176,40 6,194	1,175,39 0,417
2007	2,385,26 0,383	65,967,543	222,611,557,1 49	3,679,748, 277	47,306, 909	55,442, 956	193,05 4,015	1,352,24 7,667
2008	2,236,13 9,918	79,130,070	222,736,726,6 08	5,070,858, 236	75,918, 796	63,243, 999	153,50 5,172	1,001,91 2,242
2009	2,142,95 6,266	72,673,133	222,733,824,1 27	3,753,041, 839	73,573, 865	74,320, 182	175,80 8,767	1,034,71 8,786
2010	2,450,48 0,102	67,043,193	222,626,541,1 97	3,686,832, 140	67,076, 288	78,166, 506	204,92 8,373	1,337,19 4,629
2011	2,398,27 5,129	63,710,702	222,487,837,8 13	3,743,641, 761	47,912, 738	56,432, 877	170,45 9,783	1,404,94 3,119





2012	2,589,09	52,013,667	222,334,569,7	2,864,258,	26,234,	58,974,	223,34	1,633,46
	4,745		69	811	849	276	8,145	5,101
2013	2,269,22	64,978,113	222,458,625,7	3,700,833,	54,270,	67,961,	205,25	1,227,71
	8,484		10	331	475	698	3,614	2,022
2014	2,193,04	69,944,514	222,574,462,5	3,974,971,	44,803,	67,115,	170,74	1,220,17
	1,030		08	693	342	318	0,982	9,455
2015	2,449,70	62,201,787	222,466,595,8	3,374,434,	14,781,	64,640,	227,93	1,407,05
	2,370		16	139	188	268	7,634	2,424
2016	2,516,78	59,120,794	222,402,665,8	3,747,4429	40,697,	53,448,	220,31	1,610,08
	0,613		68	09	558	526	3,313	7,162
2017	2,273,90	80,775,412	222,688,809,4	5,228,987,	63,739,	77,841,	192,36	1,176,49
	3,311		35	865	372	432	9,477	7,385

590 The SNW has approximately 110 m of vertical relief from its highest point in the southwest corner to its outlet at the Ottawa River at its northern most point (Fig. 1A).

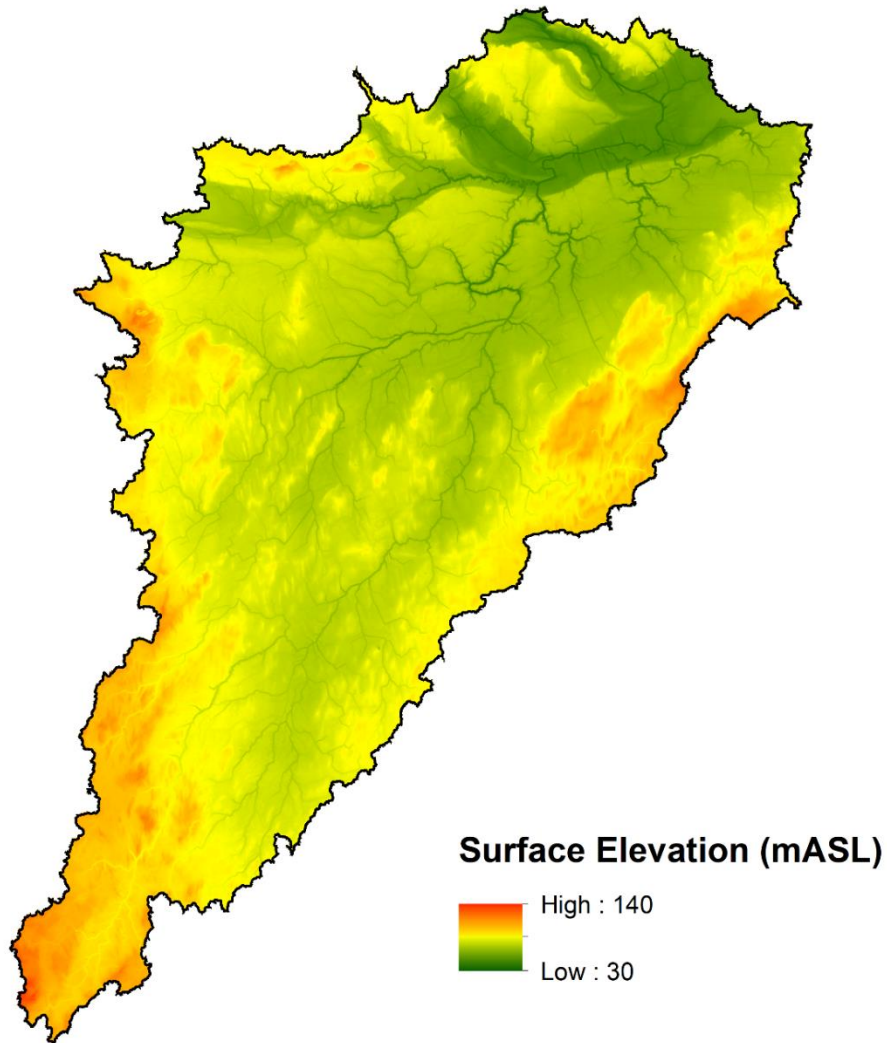


Figure 1A: Land surface elevation of the SNW

595

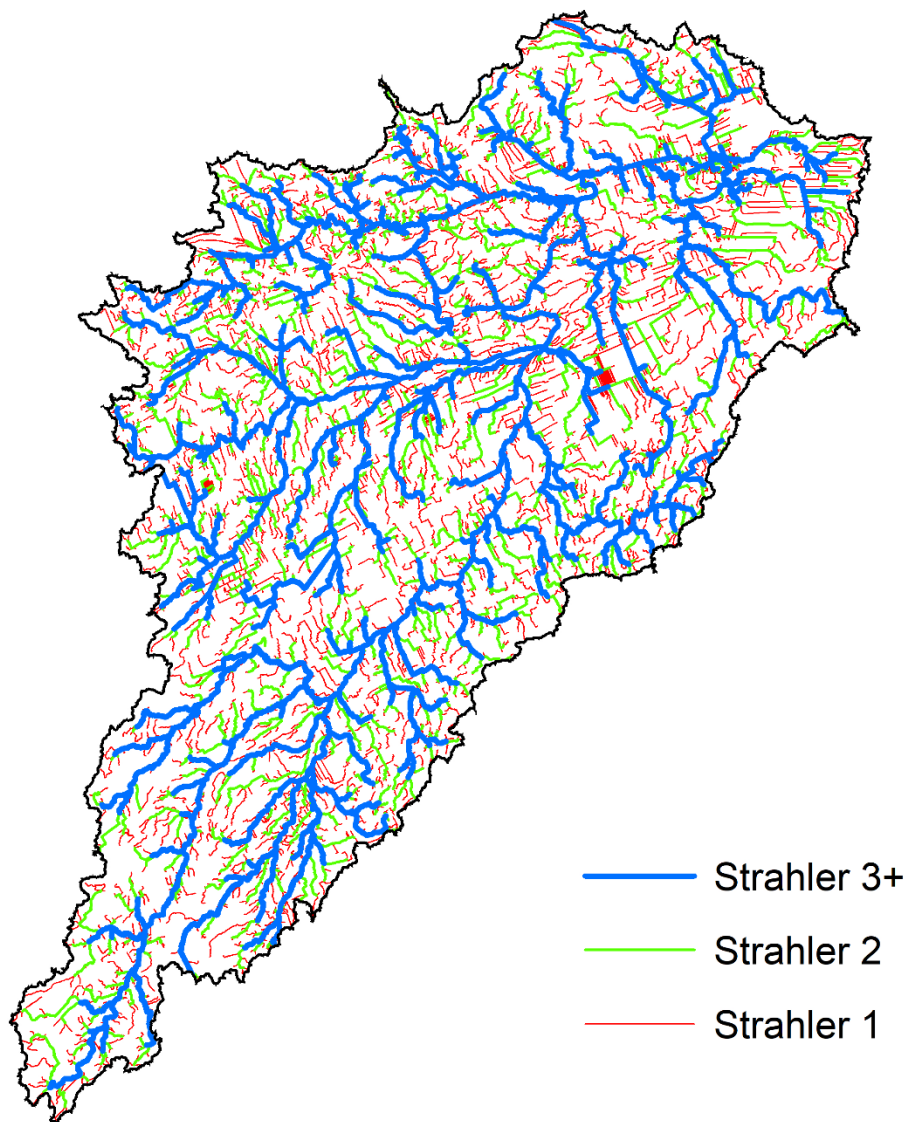
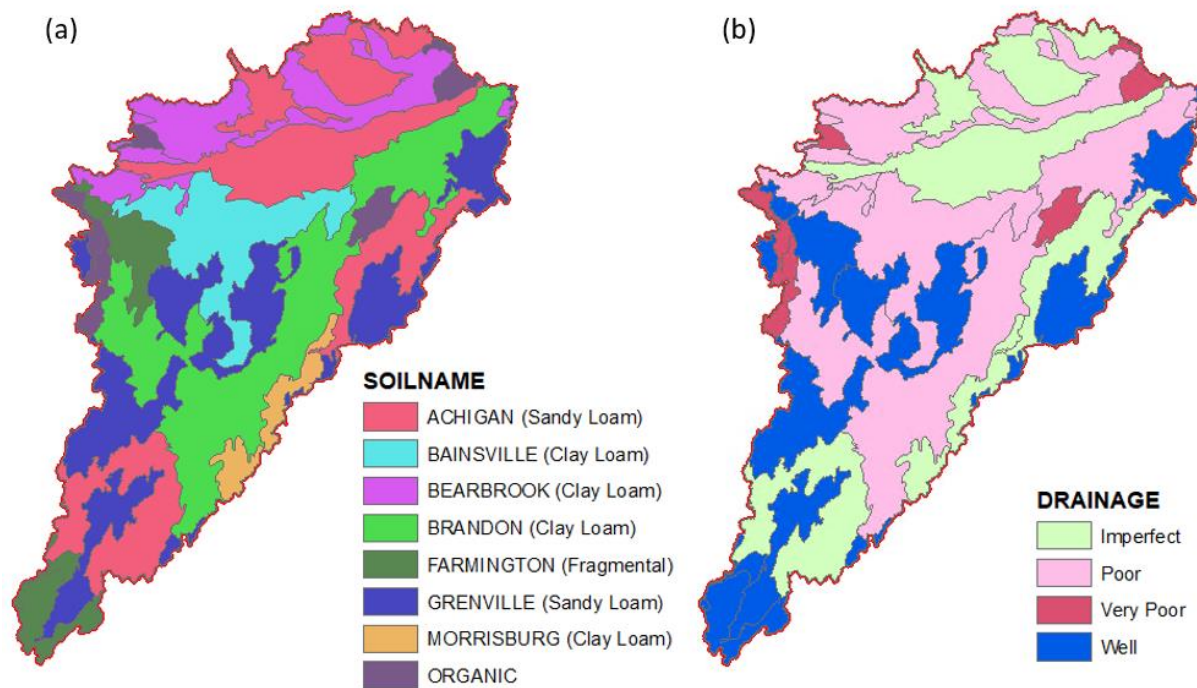


Figure 2A. Stream network distribution across the South Nation watershed, consisting of 1606 km of Strahler 3+ streams, 1548 km of Strahler 2 streams, and 3335 km of Strahler 1 streams (Ontario Ministry of Natural Resources and Forestry 2013).



600 Figure 3A. (a) Soil distribution, and (b) soil drainage status across the South Nation watershed.

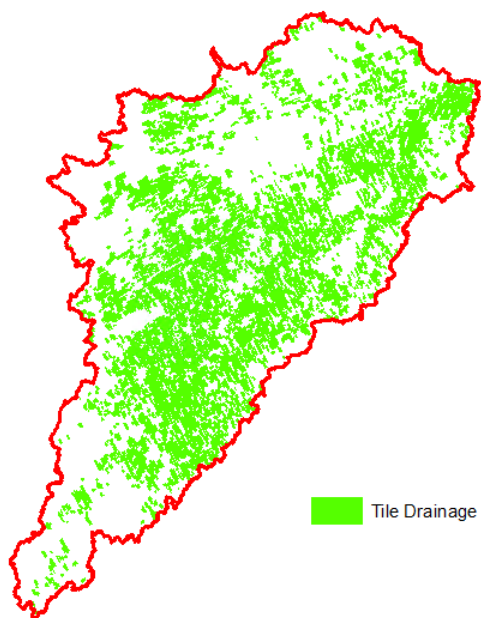
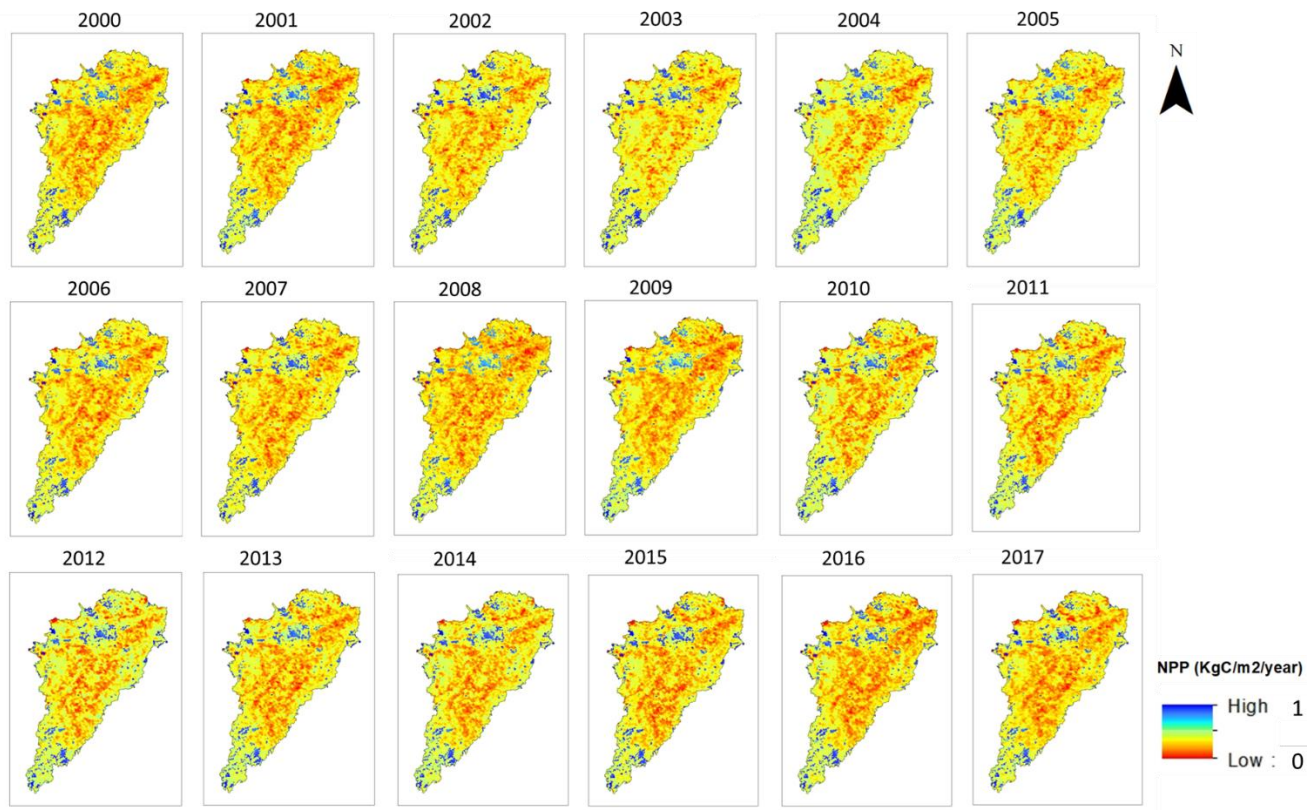


Figure 4A. Tile drainage distribution across the South Nation watershed (data provided by South Nation Conservation Authority).



605 Figure 5A: Net Primary Productivity (NPP) data for SNW (based on MODIS data).